Low-temperature electrical conductivity of highly conducting polyacetylene in a magnetic field

Y. Nogami, H. Kaneko, H. Ito, and T. Ishiguro
Physics Department, Kyoto University, Sakyo-ku, Kyoto 606, Japan

T. Sasaki and N. Toyota
Institute for Metals Research, Tohoku University, Katahira, Sendai 980, Japan

A. Takahashi* and J. Tsukamoto*
Research Association for Basic Polymer Technology, Toranomon 2-5-21, Minato-ku, Tokyo 105, Japan
(Received 19 November 1990)

The temperature dependence of the electrical conductivity and the low-temperature magnetoresistance for iodine-doped highly conducting polyacetylenes are reported. The overall behavior of the temperature dependence is explained in terms of the phenomenological Sheng model, but the selection of parameter values is not unique, suggesting that the model is not sufficient to characterize the samples. The temperature dependence changes rather drastically with the conductivity, which is determined by the doping concentration and chemical reactions within $(CH)_x$. The magnetic-field effect is rather insensitive to the field direction. This indicates that the classical orbital effect is not the principal cause. The magnetoresistance is negative for the sample with the highest conductivity, and its magnitude exceeds by far the upper bound arising from the quantum correction based on weak-localization theory for *isotropic* media. We evaluate the effect of the *anisotropy* in the electron diffusivity on the magnitude. With a decrease in conductivity, positive magnetoresistance emerges at low magnetic fields. The drastic variations of the temperature and the magnetic-field dependence with the conductivity show that the highly conducting polyacetylene is close to the metal-nonmetal transition boundary.

I. INTRODUCTION

In the past decade, conducting polyacetylene $(CH)_x$ has attracted extensive interest in both fundamental and applied research. It has the simplest backbone structure consisting of linear conjugated bonds and has been regarded as a fundamental material of conducting polymers. All the physical properties such as transport, magnetic, and optical phenomena exhibit unusual behavior, and some of them have been understood by introducing the concept of a soliton, a nonlinear elementary excitation in a quasi-one-dimensional (1D) conjugated chain.[1] The electrical-transport phenomena have not been an exception: a charged soliton, brought about by doping, works rather well to explain the electrical conduction in lightly doped $(CH)_x$. With an increase of doping level the conductivity increases further, but there are no satisfactory models to explain experimental results in this regime.

Conventional self-standing $(CH)_x$ film developed by Shirakawa and his co-workers[2] has a so-called fibril structure. It consists of a stack of a fibril and contains a large amount of vacant space ($\sim\frac{2}{3}$ of the whole volume).[2] Experimental results receive mixed contributions from intrinsic microscopic intrafibril properties and sample-dependent interfibril transfers. In some cases the latter becomes more dominant than the former: for example, the apparent dc electrical conductivity exhibits an activation-type behavior with temperature, reflecting interfibril barriers even if the fibril has a metallic nature. It seems that there will be some limit to the investigation of intrinsic intrafibril characteristics of doped $(CH)_x$ through experiments using conventional $(CH)_x$.

Recently, methods to synthesize high-density $(CH)_x$ with high-electrical conductivity have been developed.[3–5] Among them, the well-oriented $(CH)_x$ developed by Tsukamoto, Takahashi, and Kawasaki[5] yields a conductivity reaching 10^5 S/cm at room temperature which is close to the level of Cu (5.8×10^5 S/cm). The apparent density is 1.1 g/cm^3, close to the theoretical one of 1.16 g/cm^3, indicating that vacant space has been substantially removed. In this highly conducting polyacetylene (HCPA), the metallic behavior is maintained down to low temperature even in the dc electrical conductivity measurement.[6] This suggests that HCPA displays the intrinsic nature of the metallic state of $(CH)_x$ more directly than conventional forms. In other words, the essential properties of the metallic state and transport mechanism can be studied more directly through HCPA.

In this paper we present the magnetic-field dependence of the low-temperature electrical conductivity of HCPA. The behavior of the dc electrical conductivity at low temperature is indispensable in characterizing the metallic state. However, even in HCPA, observations are more or less the composite of intrafibril and interfibril properties. In order to shed light on the intrafibril nature, the magnetic field is useful since the local dynamics of the carriers is directly reflected.[7] The magnetic field also affects the interference of the carrier wave function, resulting in

some quantum corrections to the conductivity influenced by disorder[8,9]

Up to now, not a few measurements of the low-temperature electrical transport properties in heavily doped $(CH)_x$ have been reported.[10–20] The conjugated $(CH)_x$ itself is insulating due to the Peierls gap, if it is not doped. Doping with donors or acceptors results in a drastic increase in conductivity. In the lightly doped regime the nonmetallic conductivity has been interpreted on the basis of variable range hopping (VRH) of carriers, such as charged solitons, as in disordered semiconductors.[15,16,21–23] With further increase of the doping level, the formation of the metallic state has been proved by the Pauli-like magnetic susceptibility, the linear thermoelectric power, and the linear specific heat.[6,24] For heavily doped $(CH)_x$, measured temperature dependences of the electrical conductivity are analyzed phenomenologically in terms of the thermally induced fluctuation tunneling model[14,16,19,25] and/or Anderson localization,[8,9,26–31] and simply assuming that the microscopic electronic state is the ordinary (*isotropic*) one, regardless of the low dimensionality inherent in the quasi-one-dimensional (1D) conjugated structure of $(CH)_x$. We show here, using the experimental data for HCPA, that it is essential to take account of the *anisotropy* in the electron diffusivity associated with the low dimensionality. To explain the unusual metallic properties there are some exotic models such as the polaron lattice[32] and superpolaron.[33] It is expected that the nature of carriers related to the magnetoresistance should be useful to judge the soundness of these models.

II. EXPERIMENTAL

Polyacetylene films were synthesized from purified acetylene gas by the use of a catalyst aged around 200 °C in an organic solvent with a high boiling point, without adding a reducing agent. The details of the method are reported elsewhere.[5] Prior to doping, the synethesized $(CH)_x$ was uniaxially stretched by drawing. The stretching ratio was between 5 and 10 times.

Typical sample dimensions were $20\times0.8\times0.001$ mm^3. Four 25-μm-diameter Au wires were connected to samples with carbon paint as electrical contacts. The doping was performed for the *cis*-$(CH)_x$, which was converted to the *trans*-$(CH)_x$ during the process. Care was taken to reduce the contamination and the leakage of iodine dopants and the aging with oxygen. The concentration of iodine (I) dopant almost at saturation level was estimated to be 0.24 or higher for each carbon atom: $(CHI_y)_x$ where $y \geq 0.24$. The sample was mounted on a thin Kapton-film holder and covered with Apiezon-L grease in order to prevent the out-diffusion of the dopants and aging with oxygen. It was found that at room temperature conductivity gradually decreased. This was substantially suppressed by keeping samples below -10 °C.

The magnetoresistance measurements were carried out down to 0.5 K with a ^{3}He cryostat by using a Nb_3Sn superconducting solenoid magnet reaching 15 T. Four samples were installed in the cryostat so that two were in a longitudinal configuration and the others in a transverse one. Subsequent measurements were carried out after exchanging the configuration of each sample. To eliminate the effect of thermoelectric power and other noise, each datum was obtained from the difference between the values for one current direction and the other. Typical applied electric field and current were about 1 mV/m and 1 μA, respectively.

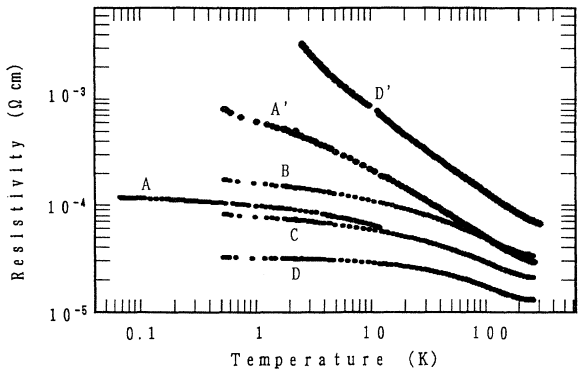

FIG. 1. Temperature dependence of the electrical resistivity of HCPA for four different samples coded A, B, C, and D and two degraded versions of A and D (represented by A′ and D′).

III. RESULTS AND DISCUSSION

A. Temperature dependence

Figure 1 shows the temperature (T) dependence of the electrical resistivity in the absence of a magnetic field for four heavily I-doped HCPA samples (coded A, B, C, and D), and two samples, (A′ and D′) degraded by keeping A and D for a week at 20 °C and for 10 days at 30 °C, respectively. The difference between samples A and D is

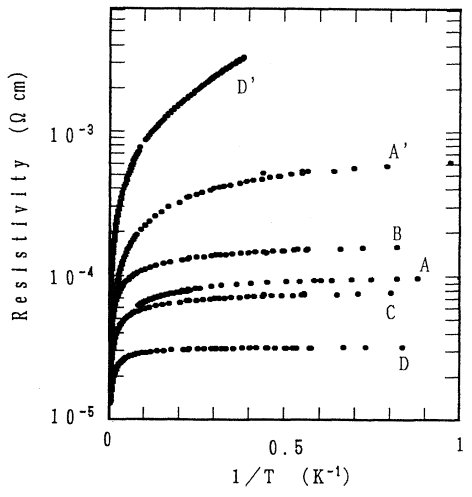

FIG. 2. Logarithmic resistivity of HCPA vs inverse temperature.

TABLE I. Lists of representative data and fitting parameters for the samples.

Sample	σ at 267 K (10^4 S/cm)	σ at 1 K (10^4 S/cm)	C (10^3 S/cm K$^{1/2}$)	σ_0 (10^4 S/cm)	λ	T_0 (K)	T_1 (K)
A′	3.39	0.163	2.10	6.23	0.06	55	180
B	2.97	0.62	1.52	4.84	0.05	90	180
C	4.73	1.29	2.24	7.49	0.05	105	180
D	7.66	3.11	2.97	14.25	0.09	120	180
D′	1.41			2.66	0.05	40	180

partly due to a slight difference in the doping level which is close to the saturation. Meanwhile the change from A to A′ and from D to D′ suggests that the difference can also be partly ascribed to degradation. As causes, we can point out three possibilities: the out-diffusion of the dopants, the chemical reaction of dopant with $(CH)_x$, and the oxidation of $(CH)_x$.

The current direction for the conductivity (σ) measurement is parallel to the stretching direction, in other words, the chain axis. The room-temperature conductivity of the samples lies between 10^5 and 10^4 S/cm. The σ versus $1/T$ plot in Fig. 2 shows that the temperature dependence cannot be fitted by activation-type behavior. Furthermore, the VRH, which is useful in lightly doped conventional polyacetylene, is not applicable except for D′ as shown in Fig. 3.

Following Thummers *et al.*[17] we plot the data on a σ versus $\sqrt{T}$ scheme as shown in Figs. 4(a) and 4(b), to see whether $\sigma(T)$ is represented by $\sigma(0)+C\sqrt{T}$, where C is a proportional constant. This temperature dependence is characteristic of Anderson localization and the electron-electron interaction mechanism in a disordered metallic system. We find that the $\sqrt{T}$ dependence is found in the temperature range below a few Kelvin; but the value of C is not universal and changes from sample to sample from 1.52×10^3 to 2.97×10^3 S cm^{-1} K$^{-1/2}$ as listed in Table I, contrary to the prediction of the model.[9] The conductivity approaches a residual value at low temperature. This suggests that the conductivity may be represented by a parallel combination of a temperature-independent (or very weakly temperature-dependent) part and a temperature-dependent part.

B. Magnetic-field dependence

The magnetic-field dependence of the conductivity was measured up to 15 T, for both the longitudinal ($\mathbf{H}\|\mathbf{j}$, H is the magnetic field, j is the current density) and the transverse ($\mathbf{H}\perp\mathbf{j}$) field configurations, in the temperature range from 0.55 to 11 K. The results are shown in Figs. 5–8,

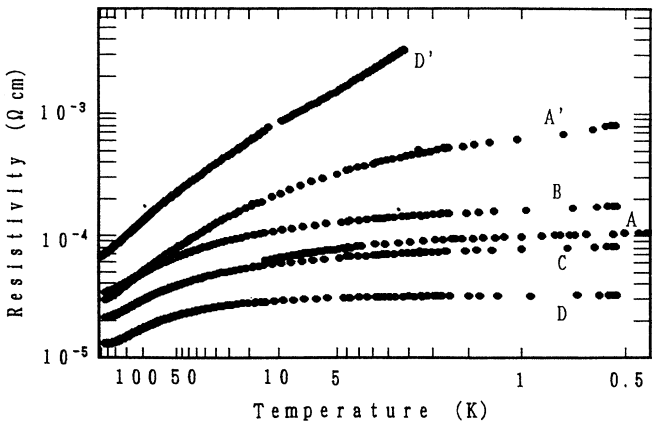

FIG. 3. Logarithmic resistivity of HCPA vs $T^{1/4}$.

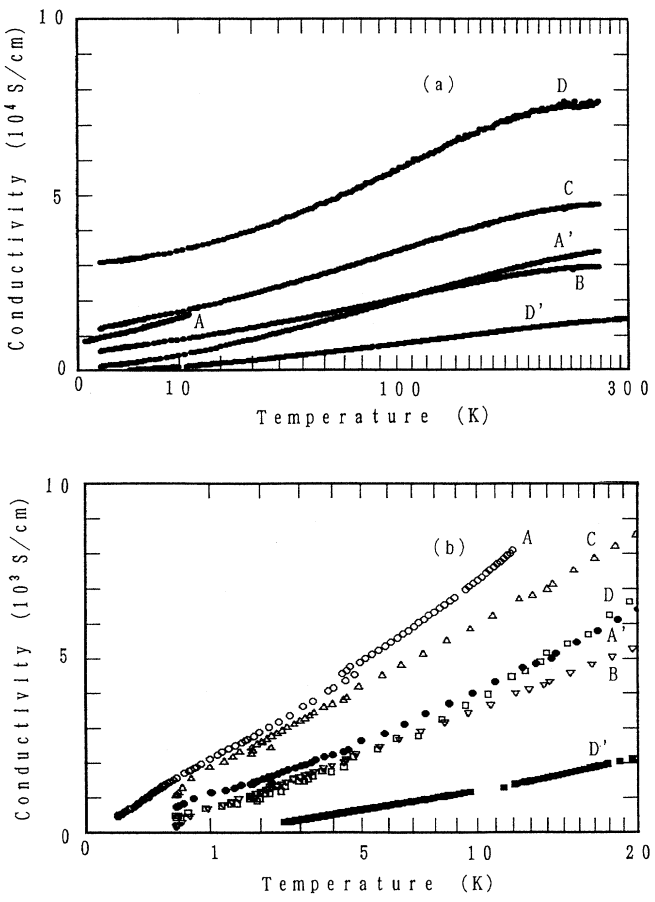

FIG. 4. (a) Conductivity of HCPA vs $\sqrt{T}$. (b) Temperature-dependent part of HCPA vs $\sqrt{T}$.

TABLE II. The zero-field conductivities at T (K), σ (T) for Figs. 5(a), 6(a), 7(b), and 8(b). The values in units of 10^3 S/cm are reduced by extrapolation of the nonzero field values.

Sample	A′	B	C	D
$\sigma(1.6)$	1.29	4.54	5.48	21.6
$\sigma(3.2)$	1.84	5.08	6.10	22.4
$\sigma(4.2)$	2.15	5.37	6.45	22.9
$\sigma(5.0)$	2.33	5.55	6.66	23.2
$\sigma(7.0)$	2.82	6.03	7.24	24.0
$\sigma(11.1)$	3.68	6.78	8.25	25.4

where we plot the shift in the conductivity $\Delta\sigma$, due to the magnetic field, for both longitudinal and transverse configurations. The conductivities in Fig. 1 represent the zero-field values for the results shown in Figs. 5(b), 6(b), 7(a), and 8(a). The zero-field conductivities for Figs. 5(a), 6(a), 7(b), and 8(b) were shifted a little as listed in Table II.

It is remarkable that the sign of the increment of the conductivity due to the magnetic field, $\Delta\sigma(H)$, is negative or positive depending systematically on the conductivity at zero magnetic field $\sigma(H=0)$ and the measuring temperature T. Sample A′, which has the lowest conductivity at low temperature among the adopted samples, is shown in Fig. 5(a) with parallel magnetic field. $\Delta\sigma(H)$ at 1.6 K changes negatively with H up to 11 T and shows a slight tendency to increase above 13 T, giving a broad minimum near 13 T, where the ratio $\Delta\sigma(13\text{ T})/\sigma(1.6\text{ K})$ reaches -0.26. The magnitude of $\Delta\sigma$ decreases at higher temperature until the sign of $\Delta\sigma$ changes at a temperature between 5 and 7 K and negative magnetoresistance is observed up to 15 T. It is also noted that the magnetic field giving minimum $\Delta\sigma$ increases with temperature. These characteristics are more clearly seen in sample C as shown in Fig. 7(a). When $\mathbf{H}\perp\mathbf{j}$ [Fig. 5(b)], $\Delta\sigma(H)$ decreases with H, reaching a minimum near 9.5 T at 1.6 K, where $\Delta\sigma(9.5\text{ T})/\sigma(1.6\text{ K})$ is -0.11. At higher temperature, above 7 K, $\Delta\sigma(H)$ becomes positive for both the longitudinal and the transverse field configurations.

On the other hand, for sample D [Figs. 8(a) and 8(b)], which has the highest conductivity among the samples, $\Delta\sigma(H)$ increases with H, in other words, the negative magnetoresistance appears, irrespective of the field direction. The value of $\Delta\sigma(H)$ increases almost linearly up to 14 T without showing any sign of saturation. For $\mathbf{H}\|\mathbf{j}$ [Fig. 8(a)], $\Delta\sigma(14\text{ T})/\sigma(0.55\text{ K})$ reaches 0.023, and the ratio decreases with increasing T but does not show a sign reversal in the measured temperature range. For $\mathbf{H}\perp\mathbf{j}$ as

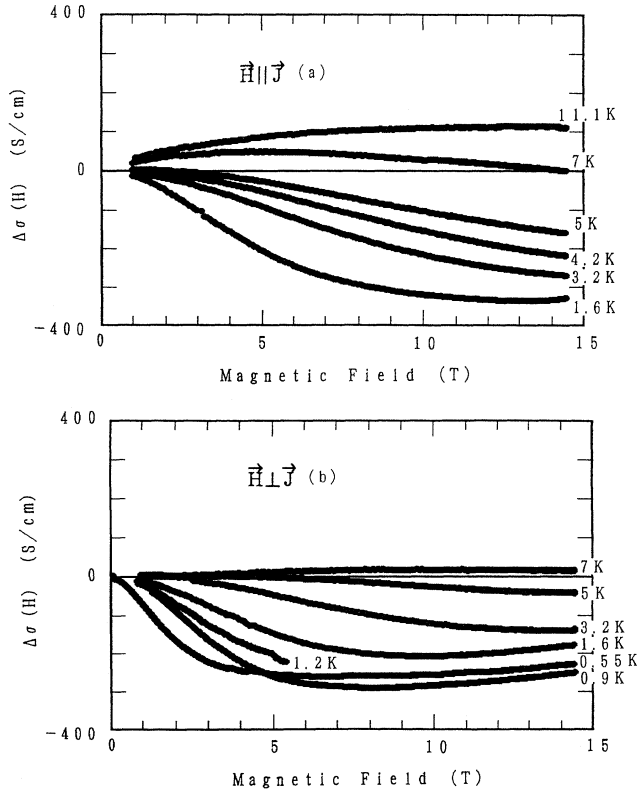

FIG. 5. Magnetic-field dependence of the conductivity increment $\Delta\sigma(H)$ at various temperatures for sample A (a) for the longitudinal field, (b) for the transverse field.

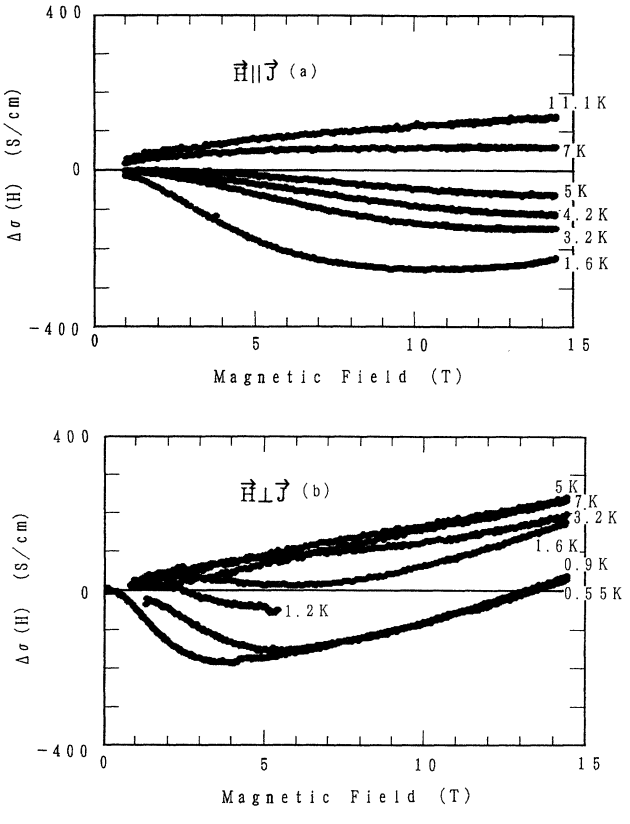

FIG. 6. Magnetic-field dependence of the conductivity increment $\Delta\sigma(H)$ at various temperatures for sample B (a) for the longitudinal field, (b) for the transverse field.

TABLE III. Comparison of $\Delta\sigma(H)/\sigma(T)$.

	Sample	A′	B	C	D
H‖j					
	$\Delta\sigma$ (14 T)/σ(1.6 K)	−0.26	−0.051	−0.013	+0.023
	$\Delta\sigma$ (14 T)/σ (7 K)	+0.001	−0.0098	+0.0048	+0.0106
H‖j					
	$\Delta\sigma$ (14 T)/σ(1.6 K)	−0.097	+0.025	+0.0059	+0.062
	$\Delta\sigma$ (14 T)/σ(7 K)	+0.005	+0.028	+0.035	+0.049

shown in Fig. 8(b), $\Delta\sigma$(14 T)/σ(1.6 K) reaches 0.062 and the ratio decreases with increase of T; again there is no sign reversal up to 11 K. For this sample, the change is larger for transverse field than for longitudinal field, contrary to the situation for sample A′.

Samples B and C, which have electrical properties intermediate between A′ and D, exhibit intermediate $\Delta\sigma(H)$, as shown in Figs. 6 and 7. For sample B with **H‖j** [Fig. 6(a)], $\Delta\sigma(H)$ is negative for low temperature but the minimum of $\Delta\sigma(H)/\sigma$(1.6 K) is seen at 10.5 T with −0.055, and the value is smaller than that for sample A′, although the sign of $\Delta\sigma(H)$ changes in the same temperature range. With **H⊥j** [Fig. 6(b)], $\Delta\sigma(H)$ shows a clear minimum at 4 T at 0.55 K and then it increases with H. In other words, the negative magnetoresistance

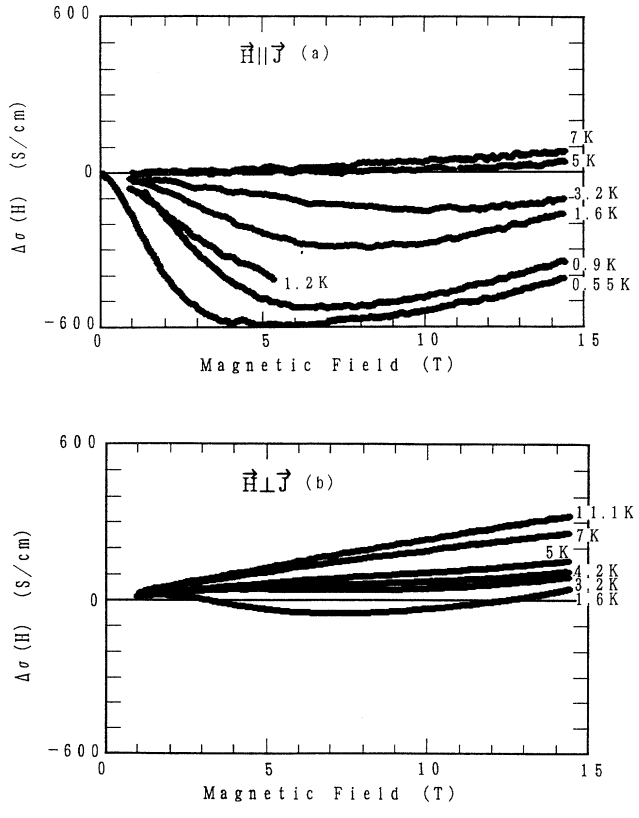

FIG. 7. Magnetic-field dependence of the conductivity increment $\Delta\sigma(H)$ at various temperatures for sample C (a) for the longitudinal field, (b) for the transverse field.

is more predominant compared with sample A′. For sample C, these features shift further so that they interpolate to sample D. For **H‖j** [Fig. 7(a)], the field giving the minimum in $\Delta\sigma$ is shifted toward lower fields and the magnitude of $\Delta\sigma/\sigma$ decreases. For **H⊥j** [Fig. 7(b)], the tendency towards linear negative magnetoresistance is enhanced.

In Table III we compare the characteristics of $\Delta\sigma(H)$ at 1.6 and 7 K, since the data at these temperatures are found in every measurement. The characteristics of the magnetic-field dependence of conductivity can be summarized as follows.

(1) The longitudinal and transverse magnetic-field cases are qualitatively similar, provided we ignore quantitative differences of a factor of at most 5.

(2) For sample D with the highest metallic conductivity, $\Delta\sigma$ increases almost linearly with H at high field region, although the slope decreases gradually with increasing T.

(3) For sample A′ exhibiting weakly nonmetallic behavior, $\Delta\sigma$ decreases with H^2 dependence at low field and then increases forming broad minimum in $\Delta\sigma$. This behavior is seen most clearly at low temperature. With further increase in H, $\Delta\sigma$ increases linearly, reminiscent of the contribution of the $\Delta\sigma(H)$ described in (2).

C. Electronic state of HCPA

As a base to understand the transport properties of the metallic $(CH)_x$, knowledge of the electronic state is indispensable. To approach this, we have measured the temperature dependence of the magnetic susceptibility $\chi(T)$ and the thermoelectric power $S(T)$ of heavily I-doped HCPA, and evaluated the electronic density of states at the Fermi energy.[6] The principal results are summarized below.

The measued $\chi(T)$ is represented by a sum of a Curie-like term and a Pauli-like term.[7] From the former, the density of paramagnetic centers coming from impurities or defects such as neutral solitons can be estimated. From the latter, the density of states at the Fermi surface, $N(\varepsilon_F)$, is found to be 0.265±0.05 states/eV C, on assumption that the electronic state is described by a degenerate electron gas model. Meanwhile, $S(T)$ is positive and almost linear in the measured temperature range 300–20 K, and the corresponding $N(\varepsilon_F)$ is estimated to be 0.19±0.03 states/eV C. A degenerate electron gas model is also supported by measurement of the electronic specific heat which is proportional to T.[34]

However, it does not guarantee the nonactivated temperature dependence down to the mK region for heavily

doped $(CH)_x$. For the quasi-1D system,[35] the strong electron localization due to disorder will prevent metallic, temperature-independent conductivity at low temperature.[31] To reconcile these observations, we consider two mechanisms. One is electron transfer between 1D polymer chains,[31–33,36] and the other is a possible violation of the localization condition due to the inelastic or spin incoherent scattering.

We should pay attention to both strong structural disorder, caused by the interruption of conjugation bonds by local chemical reactions, and the irregularity in dopant distribution. The average conjugation length for the present HCPA is estimated to be comparable to, or even a little less than, that for the conventional $(CH)_x$, according to the resonant Raman spectra.[37] The distribution of dopant is found to be rather uniform through x-ray diffraction, although this cannot rule out uncertainty in the polyiodine structure. It is shown that the relative content of I_3^- and I_5^- changes with the doping level.[38]

D. Applicability of the Sheng model and the variable range hopping

Although the magnitude of the conductivity is smaller than HCPA by at least 1 order of magnitude, metallic conductivity has been observed by the temperature-insensitive behavior at liquid-He temperatures even in the so-called Shirakawa or conventional $(CH)_x$ when the heavy doping is performed properly.[10–18] The temperature dependence, from room temperature to the liquid-He region, has been interpreted in terms of the fluctuation-induced tunneling model proposed by Sheng for disordered materials.[25] In this model, thermally activated voltage fluctuations across nonmetallic boundaries determine the temperature dependence of an aggregate of metallic strands. The dc conductivity is given by the following formulas:

$$
\begin{aligned}
&\sigma=\sigma_0\exp\{-T_1[\varepsilon^{*2}/T+\phi(\varepsilon^*,\lambda)/T_0]\}\ ,\\
&T_1=wA\varepsilon_0^2/8\pi k_B\ ,\\
&T_0=T_1/[2\chi w\xi(0,\lambda)]\ ,\\
&\phi(\varepsilon,\lambda)=\xi(\varepsilon,\lambda)/\xi(0,\lambda)\simeq\frac{1-\varepsilon}{1+\alpha\varepsilon+\beta\varepsilon^2}\ ,\\
&\alpha=4.2837\times10^{-4}(1/\lambda-4)^2\\
&\quad+4.8728\times10^{-2}(1/\lambda-4)\ ,\\
&\beta=\coth[2.6\lambda/(1-4\lambda)]-(1+\alpha)\ .
\end{aligned}
\tag{1}
$$

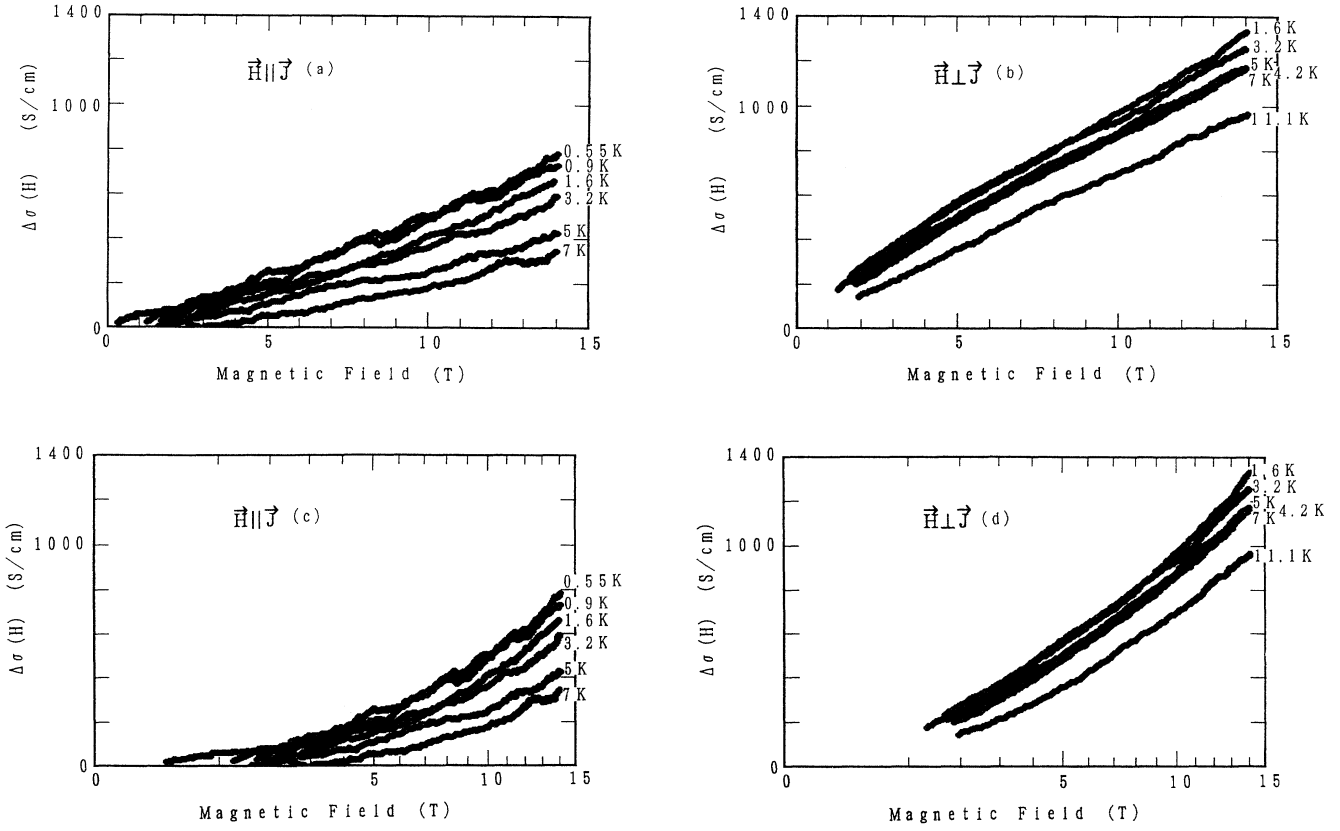

FIG. 8. Magnetic-field dependence of the conductivity increment $\Delta\sigma(H)$ at various temperatures for sample D (a) for the longitudinal field, (b) for the transverse field. (c) Plots against $\sqrt{H}$ for the longitudinal field. (d) Plots against $\sqrt{H}$ for the transverse field.

Here σ_0 is a prefactor insensitive to temperature; ε^* is the magnitude of the reduced electric field ε at the point where the exponent of Eq. (1) reaches the maximum; ε_0 is the electric field where the barrier height vanishes; k_B is the Boltzmann constant; w is the barrier width and A the junction area; λ is the image-force correction factor; and $\chi=(2mV_0/\hbar)^{1/2}$ is the tunneling constant (V_0 is the barrier height).

The experimentally measured temperature dependence of the conductivity is fitted using Eq. (1) and shown with thin lines in Fig. 9. The fitting parameters σ_0, λ, T_0, and T_1 are listed in Table I. During fitting we found that the selection of a set of the parameters is not unique, and Sheng himself has shown that the parameters and related constants are model dependent. For instance, λ and χ change with the barrier shape, which may vary depending on the way in which the sample is prepared. A larger value of λ gives more moderate temperature dependence, while selection of smaller values for T_0 and T_1 compensates this behavior and vice versa. Therefore, a choice of λ can be balanced by appropriate selection of T_0 and T_1. For example, another fitting for sample D is given by the set of values $\lambda=0.07$, $T_0=140$ K, $T_1=205$ K.

For heavily doped $(CH)_x$ exhibiting the nonactivated behavior at low temperature,[14–16] the Sheng model has been applied and the overall temperature dependence has been fitted rather well but the parameters are widely distributed as expected from the discussion above. This may partly reflect the intrinsic differences of the material and structure, but extensive effort is required to obtain a meaningful set of parameters σ_0, λ, T_0, T_1, etc. Besides the limitations we should note that resistance within the strands is neglected in the Sheng model.

We have the following remark concerning the degraded samples D′ and A′. For D′, which was the outcome of keeping sample D at 30 °C for 10 days, the metallic conduction at low temperature disappeared. The overall behavior can be fitted fairly well by the three-dimensional VRH model as shown in Fig. 3. This is understandable if we assume that the metallic strand was degraded by chemical reactions resulting in disorder in the $(CH)_x$ bonding. For A′, the level of the degradation was not the same as for D′, but the low-temperature conductivity decreased with cooling, suggesting that a transition to the nonmetallic state was beginning to occur.

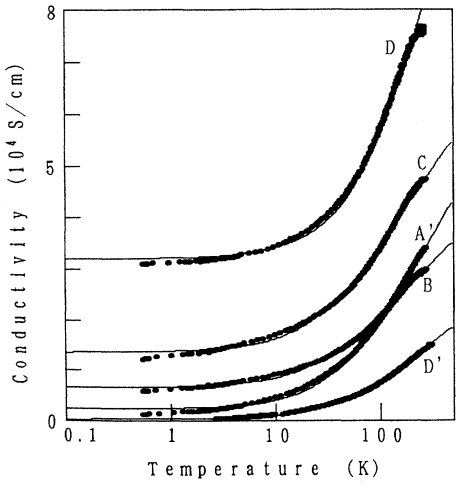

FIG. 9. Fitting of the temperature dependence by the Sheng model. Thin lines are the calculated values. The parameters are listed in Table I.

E. Effect of weak localization on magnetoresistance

The magnetoresistance gives information on the local dynamics of the charge carrier. For quasi-1D conductors, the transverse orbital motion is restricted and thereby the magnetoresistance is suppressed. This has hitherto been overlooked for conducting $(CH)_x$, and the transport phenomena in doped $(CH)_x$ have been analyzed mostly on the basis of a quasi-isotropic model. In order to get a comprehensive understanding, it is important to take account of the effect of the restricted dimensionality.

Sample A′, which has the lowest $\sigma(H=0)$ among the samples for the magnetic-field measurement, showed positive magnetoresistance increase with H^2 at low fields and a decrease above 12 and 9.5 T for the longitudinal and the transverse magnetic field at 1.6 K, respectively (Fig. 5). The H^2 term for the transverse field reminds us of the contribution from classical orbital motion, but this is not applicable in the present case since a similar effect is observed for the longitudinal field configuration. For effectively 1D conductors, the conductivity along the conducting axis should not be affected by magnetic field, since the carriers cannot make a circular motion.[39,40] As a reference, using the transport data, the value of $\omega_c\tau$ is estimated to be $\simeq 0.1$ at 15 T, where ω_c is the cyclotron frequency, τ is the scattering time of carriers, and we assume that the carrier mass is equal to the bare electron mass. Although for quasi-isotropic metal the decrement of the conductance $\Delta\sigma$ is of the order of $\sigma(\omega_c\tau)^2$, Fig. 5(b) shows that $\Delta\sigma$ at 4 T reaches as high as 20% of $\sigma(0)$ at 0.55 K. All these facts rule out classical orbital motion as the cause of the magnetoresistance.

Let us turn our attention to the most conducting sample D, which exhibits negative magnetoresistance from low magnetic field for both longitudinal [Fig. 8(a)] and transverse [Fig. 8(b)] configurations. It seems appropriate to apply the conventional arguments concerning localization which are used for disordered semiconductors and metals.[41] Although the $(CH)_x$ polymers are rather well oriented by the stretching, they form bundles of microfibrils as an aggregation of the polymers. Within the microfibrils, the length of the polymers is limited by about 10^3 CH units. With this in mind, the temperature dependence of transport phenomena of $(CH)_x$ has been analyzed in terms of either the Sheng model, or the anisotropic VRH model,[23] where the electron transfer among the metallic segments determines the overall conductivity. To interpret the magnetoresistance we should consider the local microscopic configuration which the carriers experience within their mean free length. In fact, magnetoresistance of the heavily doped $(CH)_x$ has been interpreted either in terms of VRH model[15] or weak localiza-

tion and electron-electron interaction in a disorderd system.[12,17,18,20] For samples B, C, and D the possibility of VRH conduction is ruled out by the high and temperature-insensitive conductivity.

We discuss first whether the *isotropic* three-dimensional (3D) weak localization model, which has been applied to conventional $(CH)_x$,[17,19,20] is suitable for the present case. According to 3D localization theory,[9,26,27,41] the quantum additive conductivity $\Delta\sigma_L$ due to the delocalization effects of the magnetic field and temperature (satisfying $\omega_c\tau, \hbar/\varepsilon_F\tau \ll 1$) is expressed by

$$\Delta\sigma_L(H,T)=\frac{e^2}{2\pi^2\hbar}\left[\frac{3}{2}F\left[\left(\frac{1}{4\tau_\epsilon}+\frac{1}{\tau_{so}}\right)\frac{c\hbar}{DeH}\right]-\frac{1}{2}F\left[\frac{c\hbar}{4\tau_\varepsilon DeH}\right]\right]\left[\frac{eH}{c\hbar}\right]^{1/2}+\frac{e^2}{2\pi^2\hbar}\left[3\left[\frac{1}{D\tau_{so}}+\frac{1}{4D\tau_\varepsilon}\right]^{1/2}-\left[\frac{1}{4D\tau_\varepsilon}\right]^{1/2}\right]. \quad (2)$$

Here, τ_ε is the inelastic scattering time, τ_{so} is the spin-orbit scattering time, D is the diffusion constant, and the parameter for scattering $F(x)$ is given as

$$F(x)=\sum_{N=0}^{\infty}\left[2(\sqrt{N+1+x}-\sqrt{N+x})-\frac{1}{\sqrt{N+0.5+x}}\right]. \quad (3)$$

Numerical calculation shows that $F(x)$ does not exceed 0.605.[26] The first term of Eq. (2) depends on both the magnetic field and temperature. The second term depends on temperature only through D, τ_{so}, and τ_ε. We assume that the spin flip scattering by magnetic impurities is negligible. Following from the limit on $F(x)$, there is an upper limit to the quantum correction to conductivity arising from 3D weak localization

$$|\Delta\sigma_L(H)|<4.35\sqrt{H}\ , \quad (4)$$

where H is measured in T and σ is measured in S/cm.

Since $\Delta\sigma_L(H)$ is usually positive, and independent of the field configuration, it seems appropriate to apply the correction term to explain the negative magnetoresistance for sample D. We notice, however, that the observed magnitude of $\Delta\sigma(H)$ is much larger than the upper bound predicted by Eq. (4); at 1.6 K under a transverse field of 14 T [below which the conditions to apply Eq. (2) are satisfied], the observed $\Delta\sigma(H)=1.3\times10^3$ S/cm, whereas Eq. (4) gives a value $\Delta\sigma_L\leq1.63\times10$ S/cm. This clearly indicates that the application of *isotropic* 3D localization theory is *not* suitable for the present case.

We cannot dismiss the electron interaction contribution on the magnetoconductivity. According to the interaction theory,[8] the contribution of the electron-electron interaction to the quantum additive conductivity is

$$\Delta\sigma_I(H,T)=-\frac{e^2}{4\pi^2\hbar}\left[\frac{k_BT}{2\hbar D}\right]^{1/2}\tilde{F}G\left[\frac{g\mu_BH}{k_BT}\right]. \quad (5)$$

Here, g is the g factor, μ_B is the Bohr magneton, $\tilde{F}$ is the effective screening coefficient, and $G(x)$ is defined in Ref. 8 with asymptotic form:

$$G(x)=\begin{cases}\sqrt{x}-1.3 & \text{for } x\gg1\\ 0.053x^2 & \text{for } x\ll1\ .\end{cases} \quad (6)$$

$G(x)$ increases monotonically with x, but from Eqs. (5) and (6) there is an upper bound to the magnitude of $\Delta\sigma_I$,

$$|\Delta\sigma_I(H)|\leq\left|\frac{e^2}{2\pi^2\hbar}\tilde{F}\left[\frac{g\mu_BH}{8\hbar D}\right]^{1/2}\right|. \quad (7)$$

$\Delta\sigma_I$ is usually negative when $\tilde{F}\geq0$, and its magnitude is smaller than $\Delta\sigma_L$, since HCPA has a large diffusion constant (D) of about 10^{-3} m^2/sec. In the present case, since

$$\tilde{F}\left[\frac{g\mu_BH}{8\hbar D}\right]^{1/2}\leq\left[\frac{eH}{c\hbar}\right]^{1/2}, \quad (8)$$

$\Delta\sigma_L+\Delta\sigma_I$ cannot have a large negative value. Thus the negative $\Delta\sigma(H)$ found in samples A′, B, and C cannot be ascribed to this interaction effect.

The temperature dependence of the low-temperature electronic conductivity in the metallic regime of heavily doped $(CH)_x$ has been discussed in terms of localization and interaction effects for an isotropic medium.[10–17] The second term of Eq. (2) gives the temperature dependence of $\Delta\sigma_L$ since τ_ε (the electron-phonon scattering time) is temperature dependent and represented by a power law, $\tau_e=\tau_{\varepsilon0}T^p$. This dependence of τ_ε may account for the observed $\sqrt{T}$ dependence, provided we take $p=-1$. However in that case, we notice that the coefficient estimated from Eq. (2),

$$C_T\sim\frac{e^2}{2\pi^2\hbar}\frac{1}{\sqrt{D\tau_{\varepsilon0}}}, \quad (9)$$

will be far smaller than the observed value of 1×10^3 S cm^{-1} K$^{-1/2}$ unless we assume an unrealistic value for the inelastic time coefficient $\tau_{\varepsilon0}\sim10^{-17}$ sec. According to the interaction theory, the additive conductivity $\Delta\sigma_I$ at zero field is given by

$$\Delta\sigma_I(T)=A\frac{e^2}{2\pi^2\hbar}\left[\frac{k_BT}{\hbar D}\right]^{1/2} \quad (10)$$

when $\tau_{so}\gg\tau_\varepsilon$, where A depends mainly on the carrier screening coefficient $\tilde{F}$ and has magnitude of order 1. The coefficient of $\sqrt{T}$ is evaluated to be $1.41A$ S cm^{-1} K$^{-1/2}$, and is again smaller than the experimental value of 10^3 S cm^{-1} K$^{-1/2}$ by 3 orders of magnitude.

Thus both localization and interaction models for isotropic media are unsuitable for the present HCPA. On the other hand, the magnetoresistance of the heavily

doped $(CH)_x$ has been interpreted in terms of localization and electron interaction theories[17,19,20] for the following reason. The zero-field conductivity is less by almost 2 orders of magnitude than for HCPA, so the conductivity correction due to magnetic field and temperature $\Delta\sigma(H,T)$ is similarly reduced and does not exceed the limit.

We now consider the restricted dimensionality and anisotropy of $(CH)_x$. The correction term to localization due to anisotropic diffusion constants[27,42] is given by

$$\Delta\sigma_{Lik}=\frac{D_{ik}}{D_a}\frac{e^2}{2\pi^2\hbar}\left[\frac{3}{2}F\left[\left(\frac{1}{4\tau_e}+\frac{1}{\tau_{so}}\right)\frac{c\hbar}{D_c eH}\right]-\frac{1}{2}F\left[\frac{c\hbar}{4\tau_\varepsilon D_c eH}\right]\right]\left[\frac{eH}{c\hbar}\frac{D_c}{D_a}\right]^{1/2}-\frac{D_{ik}}{D_a}\frac{e^2}{2\pi^2\hbar}\left[3\left[\frac{1}{D_\parallel\tau_{so}}+\frac{1}{4D_\parallel\tau_\varepsilon}\right]^{1/2}-\left[\frac{1}{4D_\parallel\tau_\varepsilon}\right]^{1/2}\right]. \tag{11}$$

The contribution coming from the interaction is

$$\Delta\sigma_{Iik}=-\frac{D_{ik}}{D_a}\frac{e^2}{4\pi^2\hbar}\left[\frac{k_BT}{2\hbar D_\parallel}\right]^{1/2}\tilde{F}G\left[\frac{g\mu_BH}{k_BT}\right], \tag{12}$$

where $D_\parallel$ is the diffusion constant for H parallel to the conductive axis; $D_\perp$ is that for H perpendicular; D_c is the cyclotron diffusion constant, $D_c^2=D_\perp(D_\perp\cos^2\theta+D_\parallel\sin^2\theta)$ (θ is the angle between the conducting axis and the magnetic field); D_{ik} is the diffusion coefficient tensor (for the present case $D_\parallel$); and D_a is the isotropic effective diffusion coefficient, $D_a=(\det D_{ij})^{1/3}=(D_\parallel D_\perp^2)^{1/3}$.

Comparing these formulas with Eqs. (2) and (5), one notices that the magnetic-dependent part is multiplied by $(D_{ik}/D_a)(D_c/D_a)^{1/2}$, and D is replaced by D_c in $F(x)$. The multiplication factor E is expressed as

$$E\equiv\frac{D_{ik}}{D_a}\left[\frac{D_c}{D_a}\right]^{1/2}=\begin{cases}\left[\frac{D_\parallel}{D_\perp}\right]^{1/2} & \text{for } \mathbf{H}\parallel\mathbf{j}\\ \left[\frac{D_\parallel}{D_\perp}\right]^{3/4} & \text{for } \mathbf{H}\perp\mathbf{j}\,.\end{cases} \tag{13}$$

For $(CH)_x$, we expect $D_\parallel$ along the chain to be much larger than $D_\perp$. If E is of the order of 10^2, the magnitude of the experimentally observed $\Delta\sigma$ may be explained. However, this anisotropic model has another feature in that $\Delta\sigma_L(H)$ should be anisotropic with respect to the magnetic-field direction. This arises from both E and D_c in $F(x)$ and the ratio, $\Delta\sigma_L(H\perp j)/\Delta\sigma_L(H\parallel j)$, is more than 10 for $E\cong10^2$, whereas the observed value is less than 5. Thus the anisotropic correction may explain the magnitude of $\Delta\sigma$, but it contradicts the similarity between longitudinal and transverse magnetic effects. We should, however, bear in mind the fact that the used samples are not fully oriented, and that we might not be able to dismiss the contributions from misoriented portions, which will inevitably reduce the macroscopic anisotropy appearing in the magneotresistance.

There exists a possibility that the doping realizes a quasi-two-dimensional (2D) structure, just like intercalated graphite.[43] If that is the case, one can apply the anisotropic 2D weak localization theory[42] for the present system. The additive conductivity $\Delta\sigma_L$ in the magnetic field is given by

$$\Delta\sigma_{Lik}=\frac{D_{ik}}{D_a}\frac{e^2}{2\pi^2\hbar}\left[\frac{3}{2}f_2\left[\frac{2c\hbar}{D_c eH}\frac{1}{4\tau_\varepsilon}+\frac{1}{\tau_{so}}\right]-\frac{1}{2}f_2\left[\frac{2c\hbar}{D_c eH}\frac{1}{4\tau_\varepsilon}\right]\right],\qquad f_2(x)=\log x+\varphi(\tfrac{1}{2}+1/x)\,, \tag{14}$$

where $D_a=\sqrt{D_\parallel D_\perp}$, and $\varphi(x)$ is the digamma function. Equation (14) can give both negative and positive magnetoresistance depending on the values of τ_ε and τ_{so}, but again the observed value of $\Delta\sigma(H)$ exceeds the theoretical limit if we do not take account of the multiplication factor D_{ik}/D_a. Beside this, as a whole, $\Delta\sigma_L$ in Eq. (14) has a $\log H$ dependence, in contrast to the observed H^2 or H dependence.

So far we have argued about the metallic state down to 60 mK, but we cannot dismiss the temperature dependence below 50 mK as reported by Gould *et al.*[12] Although the absolute value of σ is lower by 2 orders of magnitude compared to HCPA, the temperature dependence down to 0.1 K is similar to the present case. They claim that weak localization appears below 100 mK. It would be interesting to check whether similar behavior can be observed in the HCPA. If the magnetoresistance in HCPA is explained in terms of the effect of localization, the sources of the magnetoresistance discovered by Gould *et al.* should be an intriguing subject.

F. Relation to metal-nonmetal transition

The fact that the magnetic field and temperature dependences change strongly with the room-temperature conductivity is understandable if we remark that HCPA lies close to the metal-nonmetal boundary. Anderson localization at the boundary of the metal-nonmetal transition has been studied extensively in heavily doped semiconductors.[44] The Fermi level in these cases is close to the mobility edge. Conduction in the nonmetallic state of this regime is dominated by VRH, where the magnetic field may modify the conduction process via a Zeeman shift in the levels relevant to hopping. Electron transfers either between singly occupied levels or between doubly occupied to unoccupied and vice versa are suppressed; this results in a positive magnetoresistance.[45] Simultaneously, since the Zeeman shift acts oppositely for opposite-sense spins the mobility edge is partly lowered, so reducing the localization effect.[46] These two factors compete with each other, and the interplay in the magnetoresistance has been demonstrated in $1T$-TaS_2.[47]

Concerning the carrier concentration n_c near the metal-nonmetal boundary, we remark that $n_c\simeq10^{18}$ cm^{-3} for the heavily doped semiconductors[44] whereas

$n_c \simeq 10^{21}$ cm^{-3} for HCPA. The former is well described on the basis of the overlapping of doped impurity at its wave-function tails. On the other hand, the latter stems from the quasi-1D extended electronic state and potential disorder causing the strong scatter and/or trapping for conduction carriers. The difference in the situation at the metal-nonmetal boundary for ordinary semiconductors and for HCPA needs a revised framework to explain the magnetic-field dependences in samples A', B, and C.

IV. CONCLUDING REMARKS

The electrical conductivity of heavily I-doped HCPA reaches 10^5 S/cm at room temperature and becomes rather insensitive to temperature from 10 K down to 0.06 K. The conductivity can be suppressed either due to out-diffusion or chemical reaction of dopants, and then yields the temperature-dependent behavior. The overall characteristics from room temperature down to the liquid-helium region are explained apparently in terms of the Sheng model assuming that the conductor consists of aggregates of metallic strands. It is remarkable that the low-temperature characteristics change continuously, but drastically, from metallic to semiconducting with only a small change in the conductivity. This suggests that the metallic state is close to the metal-nonmetal transition boundary.

The low-temperature magnetoresistance in a series of HCPA samples exhibits unusual behavior, ranging from positive to negative. The variation is closely related to the conductivity in the absence of the magnetic field and its temperature dependence. Since the effect of the magnetic field is rather insensitive to the field direction, the contribution due to classical orbital motion is ruled out. Similar magnetic-field effects have been reported fragmentally and in most cases interpretation has been attempted in terms of Anderson localization for an *isotropic* medium. The present work shows definitely that this interpretation is not adequate, because the increment in conductivity obviously exceeds the upper bound arising from the quantum correction to the conductivity due to interference of scattered waves. This has not been apparent in previous observations where the sample conductivity was not so high as in the present case. The large magnitude can be explained if we take account of the *anisotropy* in the diffusion constant of carriers due to the inherent low dimensionality of $(CH)_x$. However, the observed similarity for the transverse and the longitudinal field configurations is not consistent with this anisotropic model. The contributions from misorientated parts, defects within the samples, or heterogeneous structure[48] may solve the problem, but this needs further study.

Anderson localization has been a subject of extensive investigation for thin metallic films with 2D configuration and electronic state close to the metal-nonmetal transitions, as in layered conductors and heavily doped semiconductors. Although the present HCPA is a film with thickness of the order of 1 μm, it cannot be regarded as a 2D system, but rather a bulk or 3D system with anisotropic configuration. We would like to assert that the HCPA is a categorically new system existing close to the metal-nonmetal transition boundary.

ACKNOWLEDGMENTS

We thank Professor Y. Nagaoka (Yukawa Institute for Theoretical Physics, Kyoto University) and Professor H. Fukuyama (Institute for Solid State Physics, University of Tokyo) for enlightening discussions on localization and interaction effects. We are also grateful to Professor H. Fukutome (Physics Department, Kyoto University) for stimulating discussions on the metallic state of polyacetylene. The Research Association for Basic Polymer Technology (the organization for Research and Development of Future Technology operated by the New Energy Industrial Technology Development Organization) was responsible for part of this work. The high-magnetic-field experiments were carried out at the High Field Laboratory for Superconductivity at Tohoku University.

*Mailing address: Polymers Research Lab., Toray Industries, Inc., Sonoyama 3, Otsu, Shiga 520, Japan.

[1]A. J. Heeger, S. Kivelson, J. R. Schrieffer, and W. P. Su, Rev. Mod. Phys. **60**, 781 (1988).

[2]T. Ito, H. Shirakawa, and S. Ikeda, J. Polym. Sci. Polym. Chem. Ed. **12**, 11 (1974).

[3]H. Naarmann and N. Theophilou, Synth. Metals **22**, 1 (1987).

[4]K. Akagi, M. Suezaki, H. Shirakawa, H. Kyotani, M. Shimomura, and T. Tanabe, Synth. Metals **28**, D1 (1989).

[5]J. Tsukamoto, A. Takahashi, and K. Kawasaki, Jpn. J. Appl. Phys. **29**, 125 (1990).

[6]Y. Nogami, H. Kaneko, T. Ishiguro, N. Hosoito, A. Takahashi, and J. Tsukamoto, Solid State Commun. **76**, 583 (1990).

[7]J. M. Ziman, *Principles of the Theory of Solids* (Cambridge University Press, London, 1964), Chaps. 7 and 10.

[8]P. A. Lee and T. V. Ramakrishnan, Rev. Mod. Phys. **57**, 287 (1985); in *Localization, Interaction and Transport Phenomena,* edited by B. Kramer, G. Bergmann, and Y. Bruynseraede (Springer-Verlag, Berlin, 1985).

[9]*Electron-Electron Interaction in Disordered Conductors,* edited by A. L. Efros and M. Pollak (North-Holland, Amsterdam, 1985).

[10]J. F. Kwak, T. C. Clarke, R. L. Greene, and S. B. Street, Solid State Commun. **31**, 355 (1979).

[11]Y. W. Park, A. J. Heeger, M. A. Dury, and A. G. MacDiarmid, J. Chem. Phys. **73**, 946 (1980).

[12]C. M. Gould, D. M. Bates, H. M. Bozler, A. J. Heeger, M. A. Druy, and A. G. MacDiarmid, Phys. Rev. B **23**, 6820 (1981).

[13]W. Röss, A. Philipp, K. Seeger, K. Ehinger, K. Menke, and S. Roth, Solid State Commun. **45**, 933 (1983).

[14]M. Audenaert, Phys. Rev. B **30**, 4609 (1984).

[15]E. Ettlinger, W. Schoepe, M. Monkenbusch, and G. Wieners, Solid State State Commun. **49**, 107 (1984).

[16]K. Ehinger and S. Roth, Philos. Mag. B **53**, 301 (1986).

[17]G. Thummers, U. Zimmer, F. Körner, and J. Kötzler, Jpn. J.

Appl. Phys. Suppl. **26-3**, 713 (1987).
[18]F. Komori, F. Okamoto, and S. Ikehata, in *Anderson Localization,* edited by T. Ando and H. Fukuyama, Springer Proceedings in Physics No. 28 (Springer-Verlag, Heidelberg, 1988), p. 175.
[19]Th. Schimmel, W. Riess, J. Gimeiner, G. Denninger, and M. Schwoerer, Solid State Commun. **65**, 1311 (1988)
[20]H. H. S. Javadi, A. Chakraborty, C. Li, N. Theophilou, D. B. Swanson, A. G. MacDiarmid, and A. J. Epstein, Phys. Rev. B **43**, 2183 (1991).
[21]S. Kivelson, Phys. Rev. B **25**, 3798 (1982).
[22]A. J. Epstein, H. Rommelmann, R. Bigelow, H. W. Gibson, D. M. Hoffmann, and D. B. Tanner, Phys. Rev. Lett. **50**, 1866 (1983).
[23]S. Roth, Faraday Discuss. Chem. Soc. **88**, 223 (1989).
[24]For example, A. J. Heeger, in *Handbook of Conducting Polymers,* edited by T. A. Skotheim (Dekker, New York, 1986), Vol. 2, p. 729.
[25]P. Sheng, Phys. Rev. B **21**, 2180 (1980).
[26]S. Hikami, A. Larkin, and Y. Nagaoka, Prog. Theor. Phys. **60**, 707 (1980).
[27]A. Kawabata, Solid State Commun. **34**, 431 (1980); J. Phys. Soc. Jpn. **49**, 628 (1980).
[28]H. Fukuyama and K. Hoshino, J. Phys. Soc. Jpn. **50**, 2131 (1981).
[29]C. Van Haesendonck, M. Gijs, and Y. Bryunseraede, in *Localization, Interaction and Transport Phenomena,* edited by B. Kramer, G. Bergmann, and Y. Bryunseraede (Springer, Berlin, 1985), p. 211.
[30]H. Fukuyama, Prog. Theor. Phys. Suppl. **84**, 47 (1985).
[31]L. P. Gor'kov, in *Electron-Electron Interaction in Disordered Conductors* (Ref. 9), Chap. 8.
[32]S. Kivelson and A. J. Heeger, Synth. Metals **17**, 183 (1987).
[33]H. Fukutome (unpublished). The defects in the soliton lattice carrying electronic charge is regarded as a superpolaron, H. Fukutome, J. Mol. Str. **118**, 337 (1989).
[34]D. Moses, A. Denenstein, A. Pron, A. J. Heeger, and A. G. MacDiarmid, Solid State Commun. **36**, 219 (1980).
[35]P. M. Grant and I. P. Batra, Solid State Commun. **29**, 225 (1979).
[36]A. J. Heeger, Faraday Discuss. Chem. Soc. **88**, 203 (1989).
[37]J. Tsukamoto and A. Takahashi (unpublished).
[38]T. Matsuyama, H. Sakai, H. Yamaoka, Y. Maeda, and H. Shirakawa, J. Phys. Soc. Jpn. **52**, 2238 (1983).
[39]C. Kittel, *Quantum Theory of Solids* (Wiley, New York, 1972), Chap. 12.
[40]T. Ishiguro, K. Kajimura, H. Bando, K. Murata, and H. Anzai, Mol. Cryst. Liq. Cryst. **119**, 19 (1985).
[41]S. Kobayashi and F. Komori, Prog. Theor. Phys. Suppl. **84**, 224 (1985).
[42]B. L. Al'tshuler, A. G. Aronov, A. I. Larkin, and D. E Khmel'nitskii, Zh. Eksp. Teor. Fiz. **81**, 768 (1981) [Sov. Phys. JETP **54**, 411 (1981)].
[43]G. Perego, G. Lugli, U. Pedretti, and G. Allegra, Macromol. Chem. **189**, 2687 (1988).
[44]F. Mott and M. Kaveh, Adv. Phys. **34**, 329 (1985).
[45]A. Kurobe and H. Kamimura, J. Phys. Soc. Jpn. **51**, 1904 (1982).
[46]H. Fukuyama and K. Yoshida, J. Phys. Soc. Jpn. **46**, 102 (1979).
[47]N. Kobayashi and Y. Muto, Solid State Commun. **30**, 337 (1979).
[48]A. B. Kaiser and S. C. Graham, Synth. Metals **36**, 367 (1990).